PSU/TURBO R83-2

SEMI-ANNUAL PROGRESS REPORT ON

END WALL FLOWS IN ROTORS AND STATORS OF A SINGLE STAGE COMPRESSOR

T. R. GOVINDAN, K. N. S. MURTHY AND B. LAKSHMINARAYANA

NASA GRANT NSG 3212

NATIONAL AERONAUTICS & SPACE ADMINISTRATION

LEWIS RESEARCH CENTER

TUROBMACHINERY LABOPATORY

DEPARTMENT OF AEROSPACE ENGINEERING

THE PENNSYLVANIA STATE UNIVERSITY

UNIVERSITY PARK, PA 16802

JANUARY 1983

Semi-Annual Progress Report on

END WALL FLOWS IN ROTORS AND STATORS OF A SINGLE STAGE COMPRESSOR

by

T. R. Govindan, K. N. S. Murthy, and B. Lakshminarayana

Submitted to

National Aeronautics & Space Administration
Lewis Reserach Center
21000 Brookpark Road
Cleveland, Ohio 44135

Department of Aerospace Engineering
The Pennsylvania State University
University Park, PA 16802

January 1983

PREFACE

A brief summary of the research carried out under the NASA Grant NSG 3212 during the six-month period ending December 31, 1982, is described in this report.

Section 1 reports on the progress made in developing a computer code for solving the parabolized Navier Stokes Equations for internal flows. Efforts made toward understanding and overcoming oscillations that develop in the calculation procedure take much of the discussion.

Section 2 contains a summary of the measurements being made in the hub- and annulus-wall boundary layers. This section traces the flow in the hub wall boundary layer, starting ahead of the inlet guide vanes to the inlet of the rotor.

B. Lakshminarayana

Principal Investigator

TABLE OF CONTENTS

NOMENCLATURE

C	Root blade chord of the inlet guide vane
D	Resultant flux at the present step
F	Jacobian of the convective flux vector in the normal direction
H	Jacobian of the streamwise flux vector
q	Solution vector
Δq	Delta difference of the solution vector
R	Radial distance normalized by the tip radius
SF	Shape factor, δ^*/θ
W	Axial velocity normalized by the blade tip speed
$\Delta\eta$	Normal grid step size
$\Delta\xi$	Streamwise grid step size
δ^*	Displacement thickness
θ	Momentum thickness

Subscripts

b	boundary point
1	first interior point from the boundary point b
2	second interior point from the boundary point b

1. A SPACE MARCHING SOLUTION TO THE NAVIER-STOKES EQUATIONS

The semi-annual progress report [1] for the first half of 1982 described the formulation of the space marching algorithm and its implementation. Problems encountered in implementing the scheme were mentioned. Aspects of the algorithm that required further study were the following:

1. Oscillations that developed in the solution as the calculation progressed downstream.
2. Determination of the pressure at a solid boundary.

This section of the report describes the progress made towards the solution of these problems and the status of the computer code.

1.1 Discretization of the Convective Terms

The two problems mentioned above are inter-linked and can be traced to the manner in which the first derivative terms (convective terms) were discretized in the equations. A centered difference approximation for the first derivative over three grid points involved only the outer two points and excludes the center point, the point at which the derivative is being sought. The result of this exclusion is the development of phase errors in the calculations that lead to oscillating solutions. The development and propagation of these errors have been discussed by Fromm [2]. Further, Leonard [3] shows that any such centered difference approximation for the first derivative provides no damping to damp out the errors generated, leading to growing error solutions. The suggestion by both the authors, from their studies, is the use of higher order difference schemes for the convection terms in the equations.

A different perspective to the problem is in the work of Barnett, Davis, and Rakich [3]. Consider the simple differential equation

$$\frac{dy}{dx} = f(x) \ . \qquad (1)$$

If we discretize the derivative in equation (1) with a centered difference approximation, we get

$$\frac{y_{i+1} - y_{i-1}}{2\Delta x} = f_i \ . \qquad (2)$$

Equation (2) can be solved for all of the odd-numbered grid points by stepping from the initial condition at y_1. Similarly, we can solve for all of the even-numbered grid points by stepping from the grip point y_2. However, a missing element in determining the even-grid point solution is a proper transference of the initial condition from y_1 to y_2. If this extra numerical condition is not imposed, the odd- and even-grid point solutions decouple and lead to oscillating solutions. Barnett, et al. [3] have called these extra numerical conditions as "connection" conditions and have reported considerable success from their use in eliminating oscillations.

From the above discussion we can arrive at the following conclusions in adopting a discretization for the convective derivative.

1. The commonly used centered difference approximation can lead to a decoupling of the solution at the odd- and even-grid points and subsequently lead to oscillations.
2. The use of any centered difference approximation for the first derivative provides no damping to any oscillations that may develop from the above errors.
3. Proper coupling must be provided between the odd- and even-grid points to the boundary grid points which carry the boundary condition information.

Many workers in the field have used a one-sided difference scheme to overcome some of the above problems. The scheme, while it does overcome some of the problems, is first order accurate and introduces dissipation into the scheme that is of the same order as the viscous dissipation. As shown by Leonard [2] this can lead to large errors in calculating viscous flows and should be avoided. The fourth order scheme suggested by Leonard [2] provides accurate solutions with no oscillations. The discretization can be written as

$$\frac{\partial \phi}{\partial x} = \text{sgn}(u)\left\{\frac{-\phi_{i+2}+8\phi_{i+1}-8\phi_{i-1}+\phi_{i-2}}{12\Delta x}\right\} + \left\{\frac{\phi_{i+2}-4\phi_{i+1}+6\phi_{i}-4\phi_{i-1}+\phi_{i-2}}{12\Delta x}\right\} \qquad (3)$$

where sgn(u) is the sign of the velocity that convects the first derivative. The first term in equation (3) is a centered fourth order accurate discretization of the first derivative. As mentioned above, the centered derivative provides no damping to any errors that may develop in the calculation. The second term in equation (3) provides this damping and is a fourth order derivative. Its effect is to eliminate the extreme point of the difference cell on the left or right, depending on the direction of the convective velocity, and to introduce the center point of the cell into the discretization. The overall scheme is fourth order accurate and has the same order discretization error as the error in the viscous terms.

The use of equation (3) on the explicit side of the LBI scheme poses no difficulties and with little increase in the computational effort. However, using the scheme on the implicit side results in a block pentadiagonal system that requires a considerably greater amount of computation than the inversion of a block tridiagonal system presently in the LBI

algorithm. For this reason we have decided to retain the block tridiagonal system but implement some form of "connection" conditions, as suggested by Barnett, et al. [3], to prevent solutions on the odd- and even-grid points from decoupling. This problem is acute at a solid boundary where rapid changes in the variables occur. The dominance of the second derivative viscous terms in the vicinity of a solid surface effectively "connect" all three points of the difference cell and need no further condition. It is the first derivative pressure terms that tend to decouple at the odd and even points and need further consideration. This implies consideration of the method by which the boundary conditions on the pressure are imposed at a solid boundary.

1.2 Boundary Conditions for the Pressure at a Solid Boundary

Imposing boundary conditions at a solid boundary poses no problems as far as the three velocity components are concerned. A further condition on the pressure (internal energy) is required to complete the specification of the boundary conditions. In a delta formulation of a numerical scheme, like the LBI scheme, this occurs as the delta change of the pressure on the boundary along the marching coordinate direction. This change of the pressure can be obtained from one of two equations, the streamwise momentum equation or the normal momentum equation at the boundary. The commonly used method is to use the normal momentum equation, neglecting the viscous terms as small. The simplified normal momentum equation, then, is that the normal derivative of the pressure is zero and the pressure on the boundary could be found by extrapolation from the inner pressure field. We have encountered the problem of a growing boundary pressure from this extrapolation and is possibly due to the following reasons.

As mentioned above, the use of a centered difference for the first derivative can lead to a decoupling of the solution of the odd- and even grid points. Thus, the first point away from a solid boundary, an even point, tends to develop a solution that is not constrained by the boundary value. After the inversion step, the pressure on the boundary is extrapolated from the erroneous pressure at the first even point resulting in erroneous boundary pressures. The error tends to be cumulative since the boundary pressure, due to the decoupling, cannot strongly influence the pressure at its neighboring even point.

The second option available to calculate the boundary pressure is to use the streamwise momentum equation. The use of this equation has the advantage that the pressure drop due to the shear stress at a solid boundary can be incorporated into the calculation scheme. The addition of this equation does not affect the eigenvalues of the streamwise flux vector and can be coupled to the implicit calculation scheme. However, the use of this equation on the implicit side of the calculation only decouples further the boundary grid point and the first even grid point away from it. The result is an acceptable solution on the odd grid points and a seemingly independent solution on the even grid points.

The strategy to overcome the problem, clearly, is to introduce some form of coupling between the odd- and even-grid points. This is the idea of using a "connection" condition as suggested by Barnett, et al. [3]. For this purpose we use the normal momentum equation discretized mid-point between the boundary point and the first inner point. This equation is used in addition to the equations generated at the first inner point from a three point centered discretization in the LBI scheme. This additional equation is solved for the delta difference of the pressure on the boundary in terms

of the variables at the first inner point and is substituted for in the block tridiagonal system generated by the centered three point scheme. The normal momentum equation used as a "connection" equation can be written in the form

$$\frac{H_b(\Delta q_b) + H_1(\Delta q_1)}{2} - \frac{\Delta\xi}{2}\,\frac{F_1(\Delta q_1) - F_b(\Delta q_b)}{\Delta\eta} = \Delta\xi\,\frac{D_1(q) + D_b(q)}{2} \quad . \qquad (4)$$

The centered difference of this equation at the grid point 1 can be written in the form.

$$H_1(\Delta q_1) - \frac{\Delta\xi}{2}\,\frac{F_2(\Delta q_2) - F_b(\Delta q_b)}{2\Delta\eta} = \Delta\xi\, D_1(q) \quad . \qquad (5)$$

For simplicity we have shown only the convective terms on the left-hand side of equations (4) and (5). The boundary point solution, Δq_b, can be eliminated in equation (5) using equation (4). This elimination of the boundary point also "connects" the boundary point to the first interior point. After the inversion step is completed, the boundary pressure can be found by using the streamwise momentum equation, thereby incorporating the viscous pressure drop into the calculation procedure. Further, the fourth-order scheme in equation (3) can be used on the explicit side of the calculation. This provides further transfer of information between neighboring points in the difference cell.

In summary, the scheme is implemented as follows:

1. Use a fourth-order difference scheme for the first derivative (equation (3)) on the explicit side of the algorithm.
2. Use a centered three point difference approximation on the implicit side of the algorithm along with a "connection" condition at the boundary provided by the normal momentum equation.

3. After the inversion step, use the streamwise momentum equation to calculate the pressure on the boundary.

1.3 Results

Modifications to the computer code to incorporate the techniques discussed in the previous sections have been completed and are currently being tested. Figures 1 through 5 show the secondary flow pattern development in a curved duct [5]. The overall development of the pattern is predicted well, but local regions of the flow need better prediction, particularly near the walls and in corners. Further refinement of the scheme to improve this aspect is needed and is currently being completed.

1.4 Status

It would appear at this stage that major aspects of the code development and debugging are complete. Some refinements need to be made to improve predictions in local regions of the flow. The need for further refinements will become apparent as test cases are run and analyzed. A variety of test cases will be attempted so that all aspects of the code are tested.

2. EXPERIMENTAL DATA

2.1 Hub Wall Boundary Layer Measurement

The growth of the boundary layer from upstream of the IGV to the inlet of the compressor rotor was investigated. All the measurements reported were carried out in the axial flow compressor facility. A miniature stationary five-hole probe was used for these measurements.

The radial variation of the axial velocity at different axial locations is shown in Figure 6. The variation of displacement thickness (δ^*) momentum thickness (θ) and the shape factor (SF) in the axial direction are shown in Figures 7, 8, and 9, respectively.

The flow downstream of the IGV is purely axial. This is because the turning and stagger angle of the blades at the hub are both zero. From Figures 7 and 8 it can be seen that there is a negligible boundary layer growth inside the IGV passage. This might have been caused by the favorable pressure gradient across the passage. The boundary layer grows gradually downstream of the IGV and reaches its maximum at about four chords away. This is similar to the boundary layer developing on a flat plate without the pressure gradient. But just upstream of the rotor, (about 1-1/4") both the displacement and the momentum thicknesses show a decreasing trend indicating the influence of the rotor. It seems obvious that the rotor drags the incoming boundary layer and energizes the low momentum fluid in its vicinity.

2.2 Status of Laser Doppler Velocimeter

A single channel Laser Doppler Velocimeter set-up for measurements in the compressor rotor has been completed. The set-up utilizes a TSI Model 9100 single-channel velocimeter with a 4W argon-ion laser. The

velocimeter is mounted on a traverse table that allows three degrees of linear traverse along with provision to tilt the entire assembly. Data from the velocimeter is fed into a TSI Model 1990 counter for measurement of the Doppler Frequency. Output from the counter is led to a HP 2100 Data Processing System for data logging and processing. An on-line data logging and processing program is in place on the HP 2100 to handle these tasks. The program allows for data logging using the Direct Memory Access facilities on the HP 2100 for high data transfer rates. The data processing segment of the program performs tasks like ensemble averaging of the data, data management, and also aids in proper set-up of the system for measurement. Preliminary measurements using the system are now underway.

3. PUBLICATIONS AND PRESENTATIONS

Publications:

1. "Three Dimensional Flow Field in the Tip Region of a Compressor Rotor Passage--Part 1: Mean Velocity Profiles and Annulus Wall Boundary Layer," Lakshminarayana, B., Davino, R., and Pouagare, M., Journal of Engineering for Power, Vol. 4, No. 4, pp. 760-771, October 1982.

2. "Three Dimensional Flow Field in the Tip Region of a Compressor Rotor Passage--Part 2: Turbulence Properties," Lakshminarayana, B., Davino, R., and Pouagare, M., Journal of Engineering for Power, Vol. 104, No. 4, pp. 772-781, October 1982.

3. "Development of Secondary Flow and Vorticity in Curved Ducts, Cascades, and Rotors, Including Effects of Viscosity and Rotation," Pouagare, M. and Lakshminarayana, B., Journal of Fluids Engineering, Vol. 104, No. 4, pp. 505-512, December 1982.

4. "Turbulence Characteristics in the Annulus Wall Boundary Layer and Wake Mixing Region of a Compressor Exit," Davino, R. and Lakshminarayana, B., ASME Paper No. 81-GT-148, Journal of Engineering for Power, Vol. 104, pp. 561-570, July 1982.

Presentations:

1. B. Lakshminarayana, "Turbulence Modelling and Turbomachinery Flow Computation," Workshop on Turbomachinery Flow Computation, NASA Lewis Research Center, October 21, 1982.

2. T. R. Govindan, "Space Marching Solution of Navier Stokes Equations," Workshop on Turbomachinery Flow Computation, NASA Lewis Research Center, October 21, 1982.

REFERENCES

1. Govindan, T. R., Lakshminarayana, B., and Murthy, K. N. S., "End Wall Flows in Rotors and Stators of a Single Stage Compressor," Semi Annual Progress Report, NASA Grant NSG 3213, July 1982.

2. Fromm, J. E., "Numerical Solution of the Navier-Stokes Equations at High Reynolds Numbers and the Problem of Discretization of Convective Derivatives," AGARD Lecture Series No. 48, 1972.

3. Leonard, B. P., "A Survey of Finite Difference With Upwinding for Numerical Modelling of the Incompressible Convective Diffusion Equation," in Computational Techniques in Transient and Turbulent Flow, Edited by C. Taylor and K. Morgan, Pineridge Press, 1981.

4. Barnett, M., Davis, R. T., and Rakich, J. V., "Implicit Boundary Conditions for the Solution of the Parabolized Navier-Stokes Equations for Supersonic Flows," NASA CP 2201, 1981.

5. Taylor, A. M. K. P., Whitelaw, J. H., and Yianneskis, H., "Measurements of Laminar and Turbulent Flow in a Curved Duct with Thin Inlet Boundary Layers," NASA CR-3367, 1981.

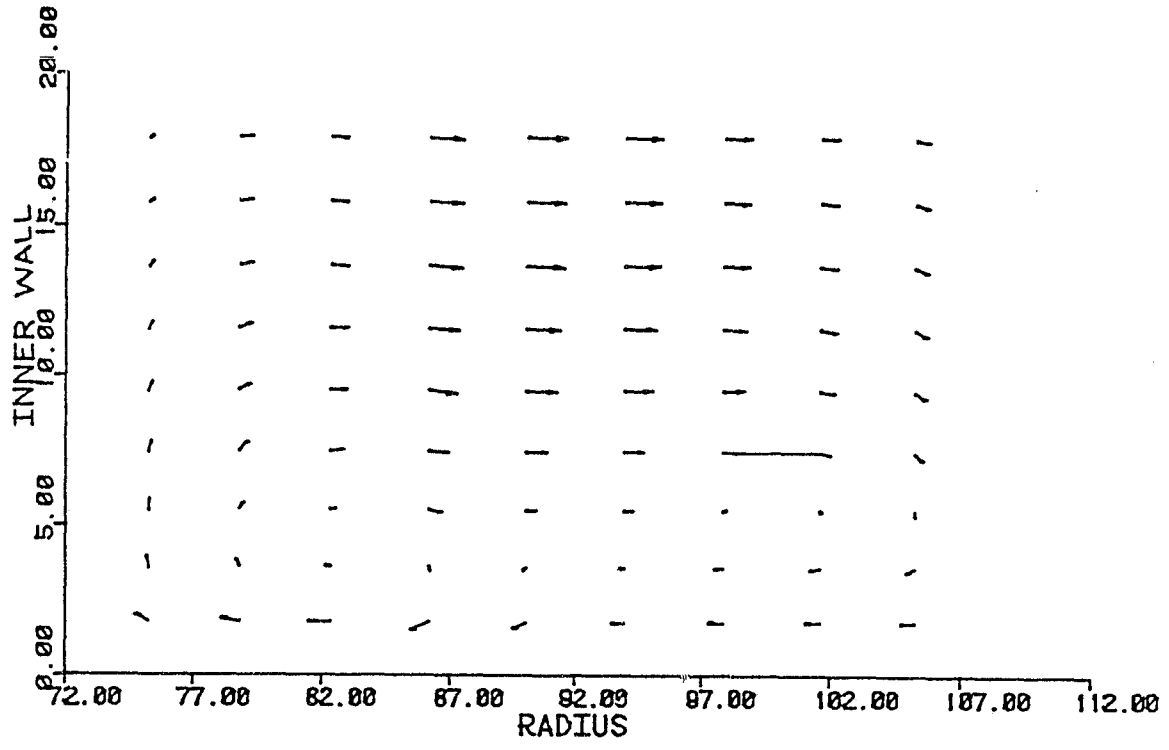

Figure 1. Secondary Flow at 8° Turning

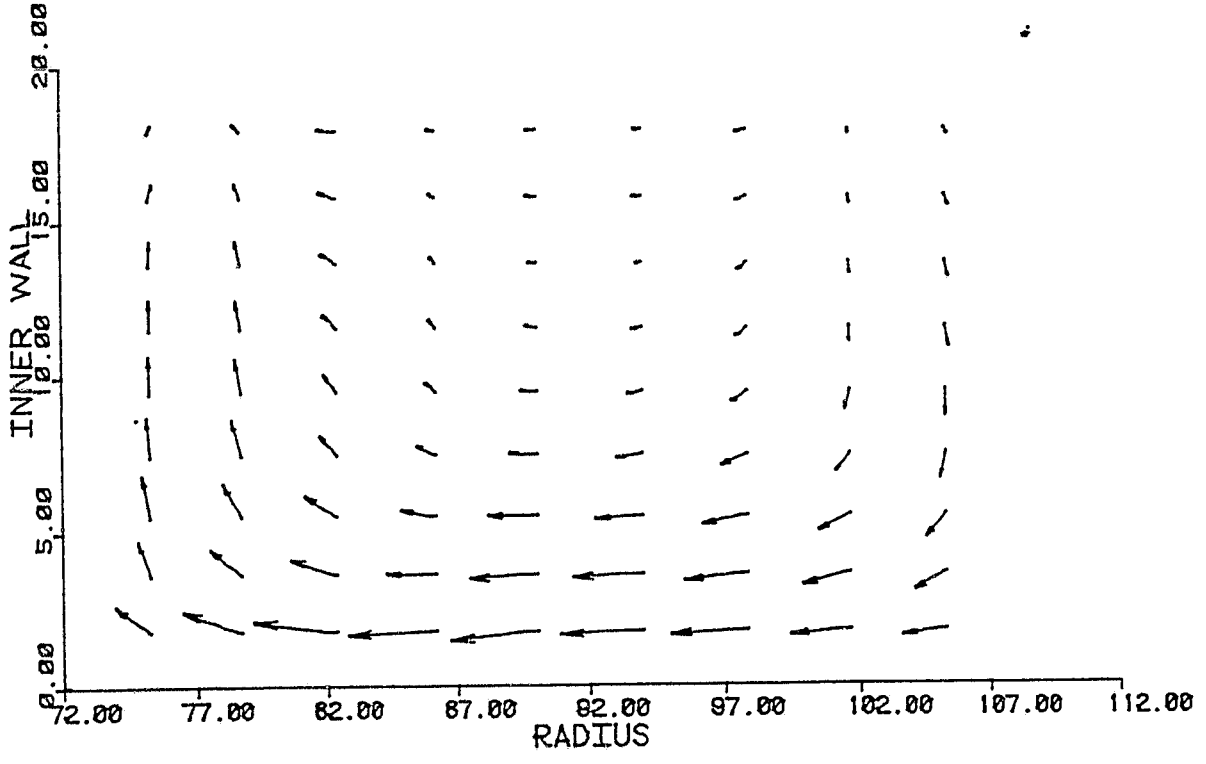

Figure 2. Secondary Flow at 16° Turning

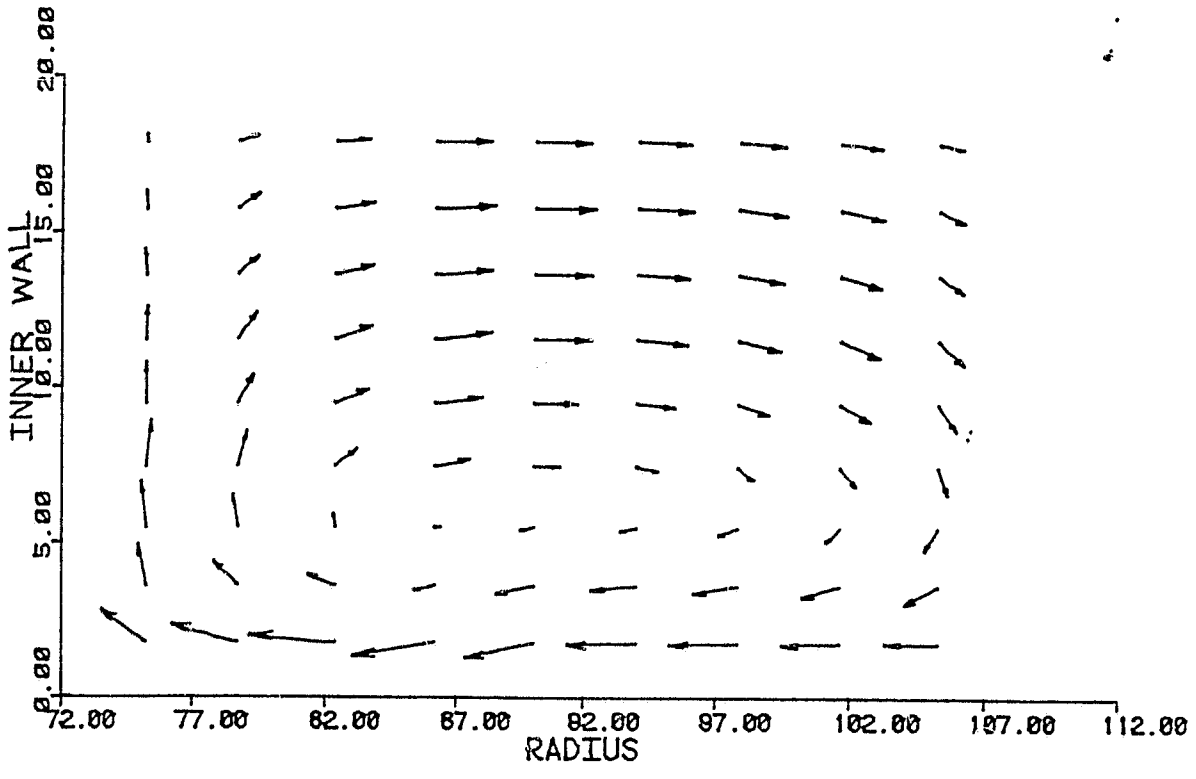

Figure 3. Secondary Flow at 24° Turning

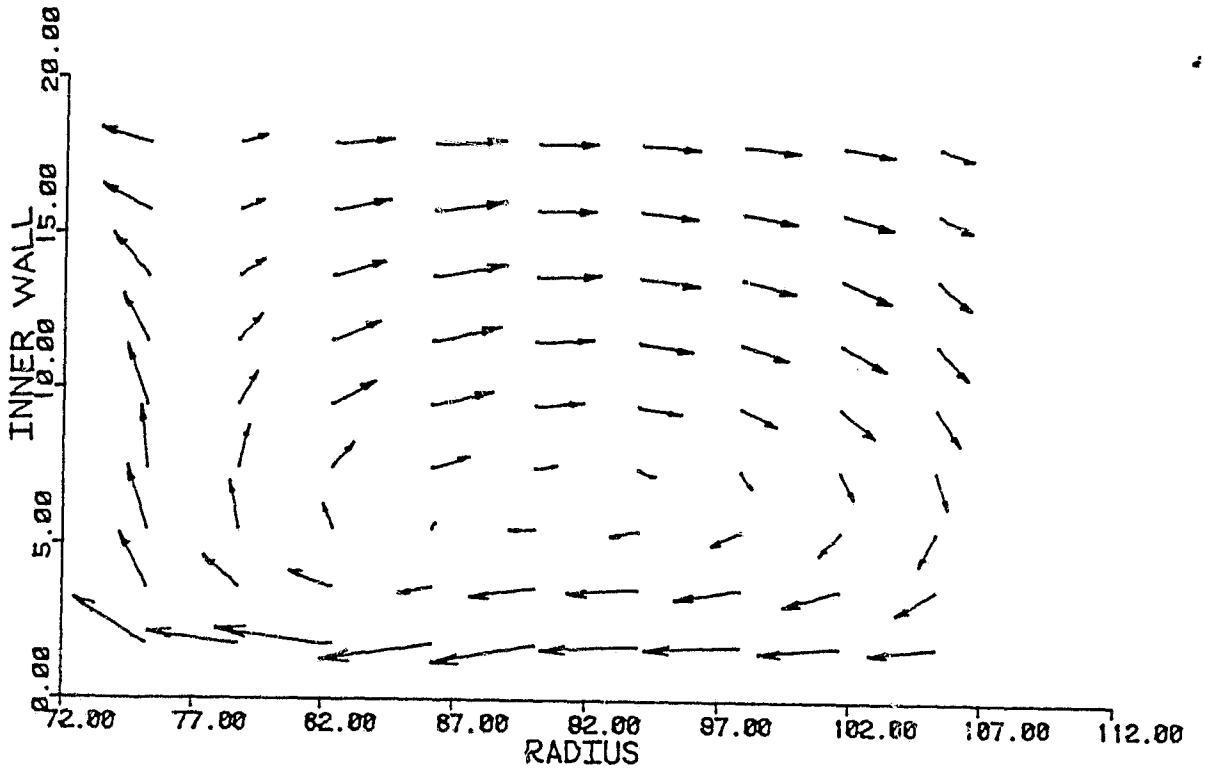

SECONDARY FLOW VECTORS AT STATION 80

Figure 4. Secondary Flow at 32° Turning

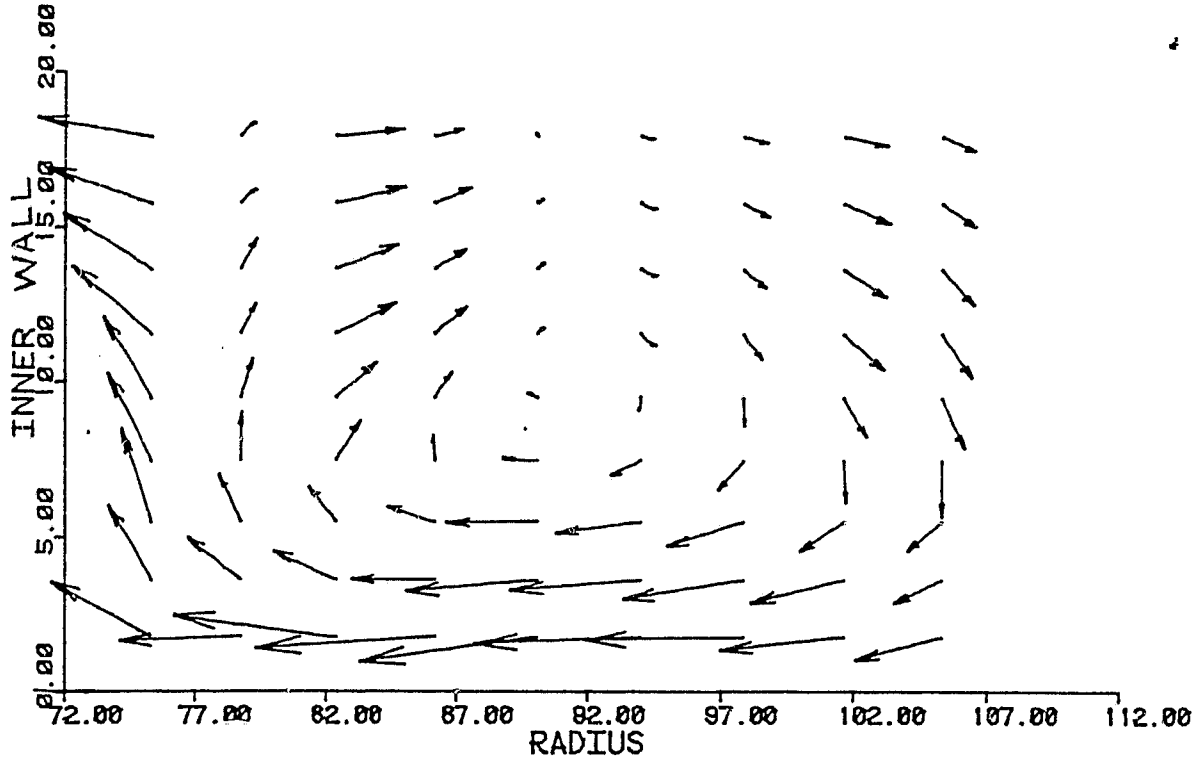

SECONDARY FLOW VECTORS AT STATION 100

Figure 5. Secondary Flow at 40° Turning

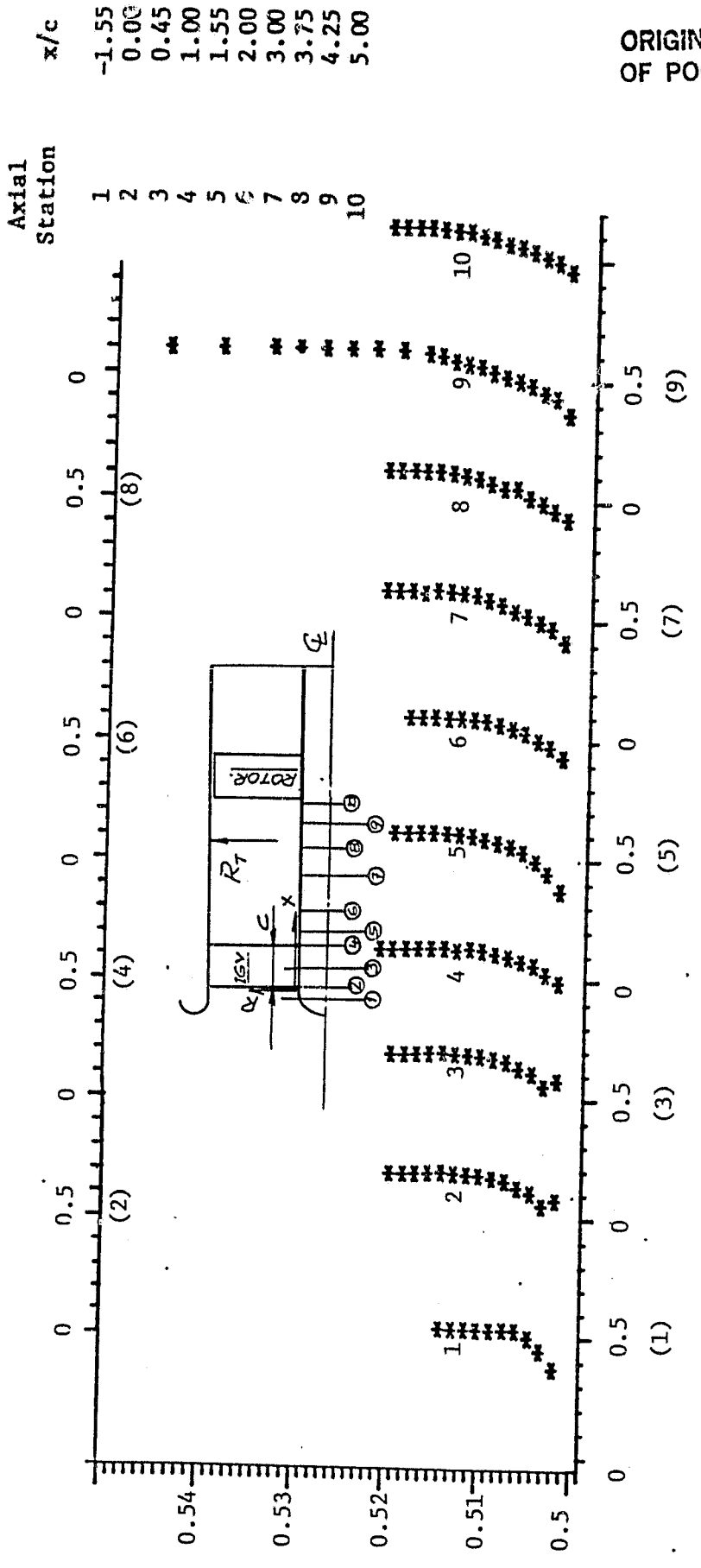

Figure 6. Radial Variation of Axial Velocity at Different Axial Locations

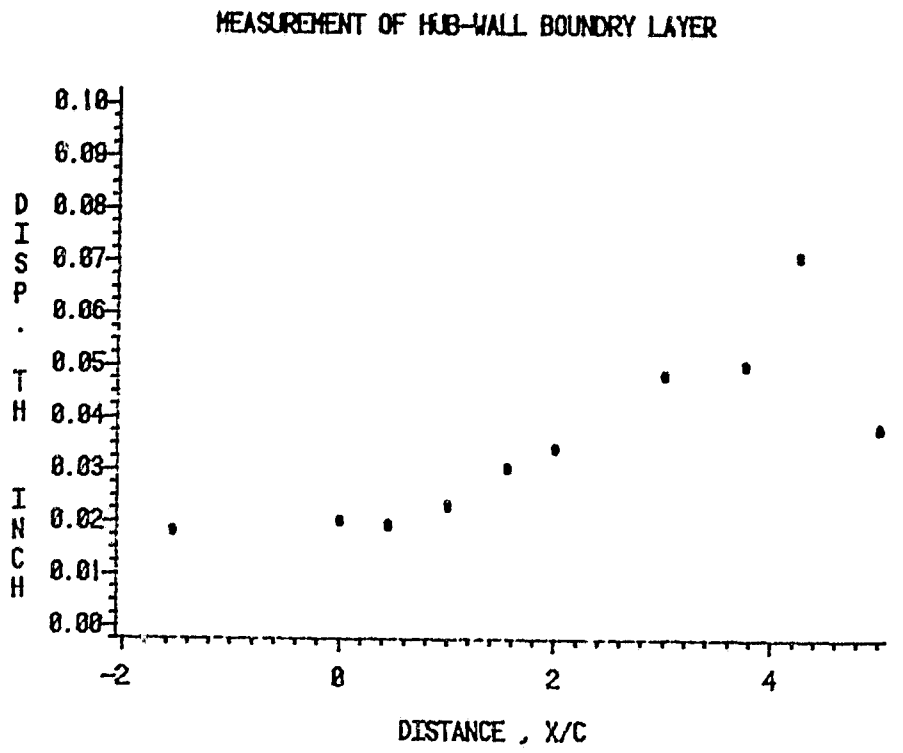

Figure 7. Variation of Displacement Thicknessin the Axial Direction

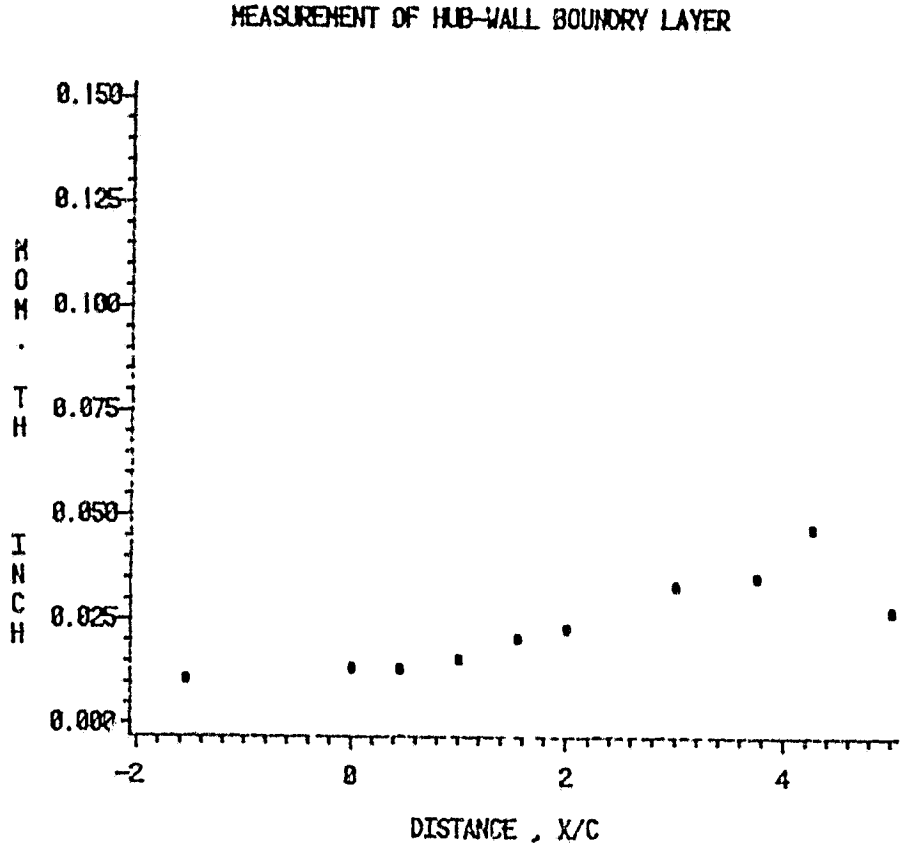

Figure 8. Variation of Momentum Thickness in the Axial Direction

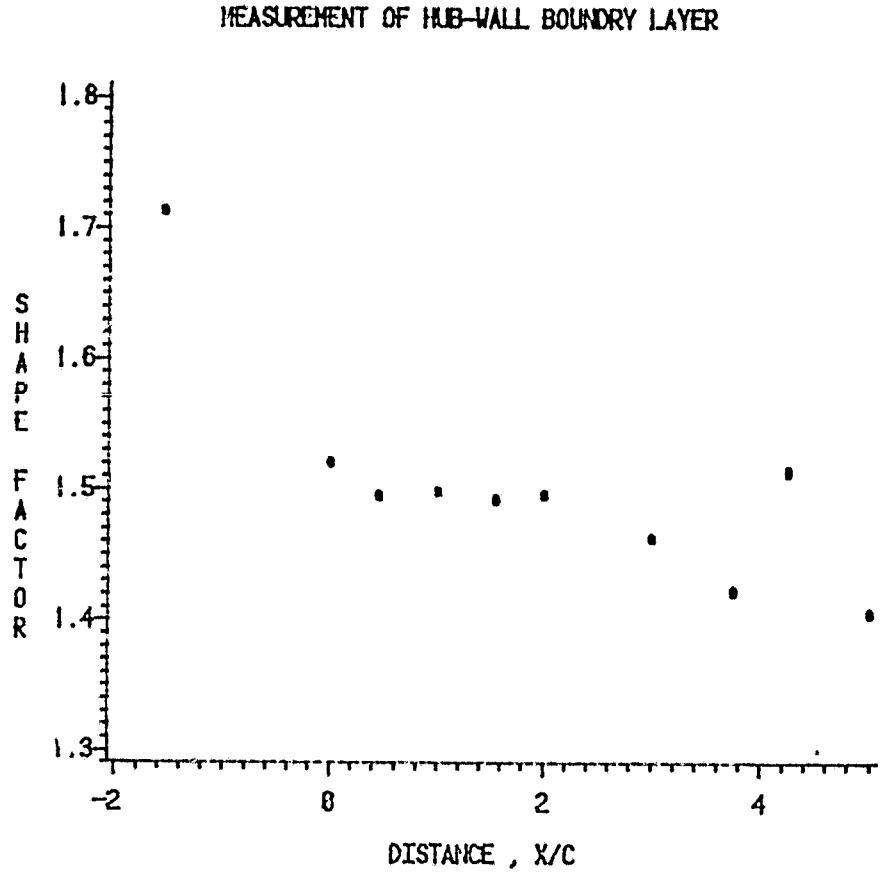

Figure 9. Variation of Shape Factor in the Axial Direction